Straum, I. L., C. Sindland, V. Andersen, and V. Myrvågnes. 2026. High-Temperature Behaviour of Quartz-Charcoal Briquettes in Metallurgical Silicon Production. In *Silicon for the chemical and solar industry XVIII,* edited by M. Tangstad, H. Rong, A. Valderhaug, B. Andresen, H. Dalaker, and I. G. Page. Kristiansand, Norway, September 7–10, 2026. https://doi.org/10.55669/oa900832

High-Temperature Behaviour of Quartz–Charcoal Briquettes in Metallurgical Silicon Production

I.L. Straum[1], C. Sindland[1,2], V. Andersen[2], and V. Myrvågnes[1,2]
[1]Department of Materials Science and Engineering, NTNU, Norway
[2]Elkem ASA, Norway

Keywords: Fines utilization, Agglomerates, Biocarbon, Silicon Production, SiO-reactivity, SiC-formation

Abstract – The high-temperature behaviour of quartz–charcoal briquettes (QCB) and reference charcoal briquettes (CB) was investigated under conditions relevant to metallurgical silicon production. QCB briquettes contained 30 wt.% quartz, 60 wt.% calcined charcoal, and 10 wt.% corn starch binder. Briquettes were heat treated at temperatures between 1400°C and 2000°C, both with and without exposure to externally generated SiO(g), and characterised by thermogravimetric analysis (TGA), X-ray diffraction (XRD), scanning electron microscopy (SEM), image analysis, apparent and envelope density measurements, and off-gas analysis. An initial mass loss of approximately 13 wt.% was observed below 900°C, attributed to binder decomposition, devolatilisation, and moisture removal. SiC formation started at 1400°C, below the thermodynamic equilibrium onset of approximately 1500–1520°C. The main carbothermal reduction stage occurred between 1400°C and 1700°C, during which all crystalline silica phases were consumed and total SiC content reached approximately 22 wt.%, consistent with the theoretical value for complete quartz conversion. The CB briquettes showed no significant phase development in the absence of quartz. Exposure to externally generated SiO(g) resulted in additional SiC formation concentrated at the bottom and sides of both briquette types, and the QCB briquettes retained significant SiO-capture capability after extensive internal reduction. The results demonstrate that composite quartz–charcoal briquettes are reactive under silicon production conditions and show potential for improved utilisation of fine raw material fractions.

1. INTRODUCTION

Silicon is produced industrially through carbothermic reduction of quartz in a submerged arc furnace (SAF), using carbonaceous reductants such as coal, coke, charcoal, and wood chips. The simplified overall reaction is shown in *Equation 1*, although in practice several reactions and phase transformations occur at different temperatures and furnace zones (Schei et al., 1998).

$$SiO_2 + 2C \rightarrow Si + 2CO \quad [1]$$

An important operational challenge is the generation and handling of fine raw material fractions. Fine particles are produced during quartz mining and during the production, transport, and handling of carbonaceous materials. When charged directly to the furnace, fines may reduce charge permeability, disturb upward gas flow, and contribute to unstable furnace operation (Ringdalen et al., 2022; Haugedal, 2025). Fine carbon particles, particularly fractions below 1 mm, may also be carried with the furnace off-gas and subsequently combust in the

furnace hood or off-gas system, resulting in reductant losses and changes in the carbon balance (Schei et al., 1998).

Agglomeration has been proposed as a route for converting fine quartz and carbon fractions into raw materials with improved properties for furnace use (Schei, 1998; Li, 2017; Kyaw, 2024). By combining quartz and carbon within the same briquette, closer contact between reactants may be achieved while maintaining sufficient permeability in the furnace charge (Li, 2017). Composite agglomerates may also influence local reactions involving SiO(g) and alter the reaction behaviour within the charge.

The close contact between quartz and charcoal particles within the briquette reduces the transport distance for gaseous intermediates and may therefore alter the effective reaction kinetics compared with a conventional loose furnace charge. Wiik (1990) demonstrated experimentally that the reaction between solid silica and solid carbon proceeds primarily via the gas phase rather than as a direct solid–solid reaction, as described in *Equations 2* and *3*. These two reactions combine to give the overall SiC-forming reaction shown in *Equation 4*. This two-step gas-phase mechanism was confirmed by Li (2017), who identified it as the dominant reaction path in the SiC-producing stage of quartz–carbon pellets in both CO and Ar atmospheres.

$$SiO_2 + C = SiO_{(g)} + CO \quad [2]$$

$$SiO_{(g)} + 2C = SiC + CO \quad [3]$$

$$SiO_2 + 3C = SiC + 2CO \quad [4]$$

Although thermodynamic equilibrium calculations predict that the conversion of SiO_2 and C to SiC becomes favourable at approximately 1500–1520°C, Poch and Dietzel observed the onset of SiC formation already at 1350°C in an argon atmosphere (Poch and Dietzel, 1962). This suggests that the close contact of reactants in a composite briquette, combined with the locally reducing gas atmosphere, may further facilitate SiC formation below the thermodynamically predicted onset temperature.

This paper presents results from an experimental investigation of quartz–charcoal briquettes (QCB) heat treated at temperatures between 1400 °C and 2000 °C, both with and without exposure to externally generated SiO(g). The objective was to characterise the reaction behaviour, phase development, and microstructural evolution of composite briquettes relevant to MG-Si and FeSi production.

2. EXPERIMENTAL

2.1 Materials and briquette preparation

Two briquette compositions were investigated. QCB contained 30 wt.% quartz, 60 wt.% calcined charcoal, and 10 wt.% corn starch binder. Reference CB contained 90 wt.% calcined charcoal and 10 wt.% binder. The quartz was dried at 105°C, sieved to 100–250 µm, and characterised by XRF analysis, which showed approximately 99 wt.% SiO_2 with minor impurities.

Two batches of the same charcoal were calcined at 900°C (Batch 2) and 1200°C (Batch 1) to remove PAH-containing volatile matter. After calcination, both batches showed fixed carbon

contents of approximately 94 wt.% (dry basis), ash contents of 4.3–4.9 wt.%, and residual volatile matter of 1.4–1.5 wt.%, as determined by proximate analysis.

Briquettes were prepared by mixing charcoal and quartz with a gelatinised binder paste (corn starch mixed with water), pressed into cylindrical pellets (10 mm diameter, ~12 mm height for CB and ~10 mm for QCB), and dried at 105°C for 24 hours. The binder content of 10 wt.% refers to the dry component mixture; water was added only to facilitate gelatinisation and was largely removed during pressing and drying. A total of 252 briquettes were produced across 21 experimental batches, with batches consisting of 12 briquettes of identical composition and a total dry mass of approximately 10 g.

2.2 High-temperature experiments

Heat treatment was performed in a graphite tube resistance furnace under inert atmosphere (Ar below 2000°C and He at 2000°C to reduce the risk of argon ionisation). Standard experiments used a heating ramp of approximately 40 minutes to the target temperature followed by a 30-minute isothermal hold, except at 1450°C where a 2-hour hold was used to assess time-dependent conversion. Target temperatures were 1400, 1450, 1700, 1900, and 2000°C.

Selected experiments included exposure to externally generated SiO(g). A Si–SiO_2 mixture (0.5–1 mm particle size) placed in a lower crucible within the same furnace assembly served as the SiO source, as shown in *Figure 1*. Off-gas CO and CO_2 concentrations and temperature were monitored continuously throughout all experiments.

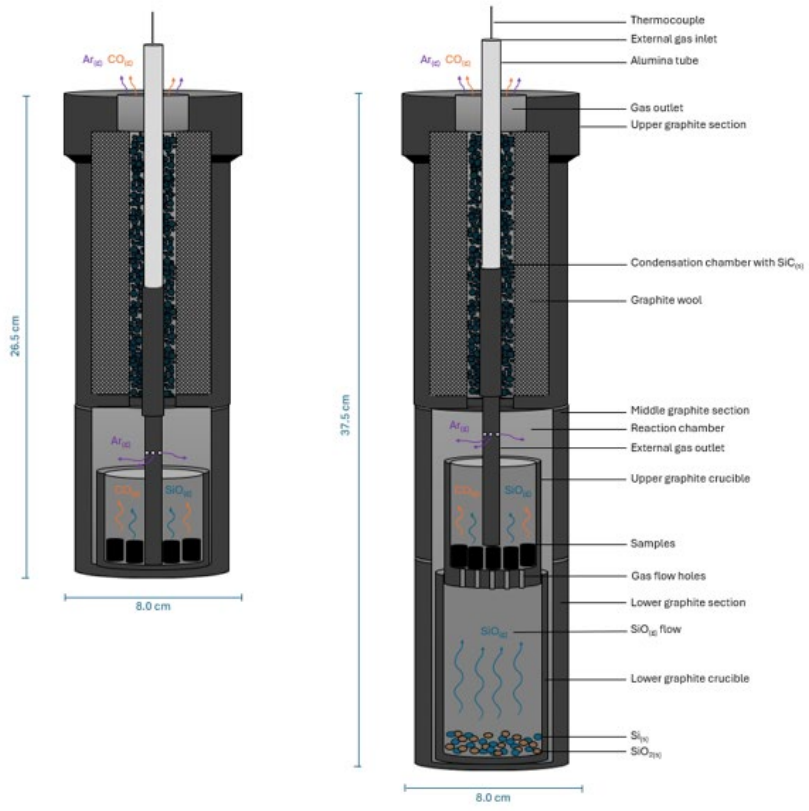

Figure 1: Schematic illustration of the standard furnace setup (left) and the SiO(g) exposure setup (right), showing the graphite crucible assembly, sample placement, and gas flow directions.

2.3 Characterisation

Phase evolution was characterised by XRD. Microstructural development was examined by BSE-SEM, in which contrast distinguishes quartz (bright), SiC (intermediate), and carbon (dark) based on mean atomic number. Each briquette cross-section was reconstructed from approximately 20–40 individual BSE-SEM images. Phase area fractions were quantified from the reconstructed images using a custom Python script applying Otsu-based thresholding. Apparent density and envelope density were determined by Archimedes' method and a GeoPyc analyser, respectively. TGA experiments (50°C/min to 1500°C) were performed to characterise binder decomposition independently of the high-temperature reactions.

3. RESULTS AND DISCUSSION

3.1 Expected reaction sequence

Before presenting the experimental results, it is useful to establish the theoretically expected reaction sequence. *HSC Chemistry* equilibrium calculations for the QCB composition (30 wt.% quartz, 60 wt.% charcoal) predict that SiO_2 remains stable up to approximately 1500–1520°C, above which SiC and CO(g) are formed according to *Equation 4*. Assuming a SiO partial pressure of 1 bar, significant SiO(g) formation from the Si–SiO_2 lower crucible is predicted above approximately 1930–1940°C, consistent with the findings of Sindland (2020), who reported weight losses of 45–50 wt.% from Si–SiO_2 mixtures at 1930–1950°C for a 30-minute hold.

Based on the QCB composition (30 wt.% quartz, 60 wt.% charcoal) and the SiC-producing reaction (*Equation 4*), complete internal carbothermal reduction of the quartz fraction is expected to yield approximately 20 wt.% SiC, with a corresponding CO-related mass loss of approximately 28 wt.%. If 1 g of externally generated SiO(g) additionally reacts with carbon according to *Equation 3*, the expected total SiC content increases to approximately 29 wt.%. These theoretical values provide reference points for interpreting the experimental XRD and mass-loss results.

The expected mass development during heating is illustrated in *Figure 2*. The initial mass loss below approximately 400°C corresponds to decomposition of the binder, residual moisture, and residual volatile matter in the charcoal. The corn starch binder contributes approximately 9.4 wt.% volatile loss when used at 10 wt.% addition (Kyaw, pers. comm., 2026), while the remaining contribution was estimated from the measured moisture and volatile matter contents of the calcined charcoal. This resulted in theoretical low-temperature mass losses of 12.58 wt.% for CB and 11.65 wt.% for QCB. For the QCB briquettes, a further mass loss is expected between approximately 1500°C and 1700°C due to CO(g) evolution accompanying SiC formation. In the SiO-exposure experiments, additional SiC formation from externally supplied SiO(g) above approximately 1930°C may partially offset this mass loss, resulting in an increase in remaining briquette mass relative to the standard experiments. The curves for 25% and 50% SiO utilisation represent scenarios where 25% and 50%, respectively, of the experimentally estimated SiO(g) generated during each experiment (approximately 3.8 g for CB and 5.7 g for QCB) is assumed to react with carbon in the briquette to form SiC.

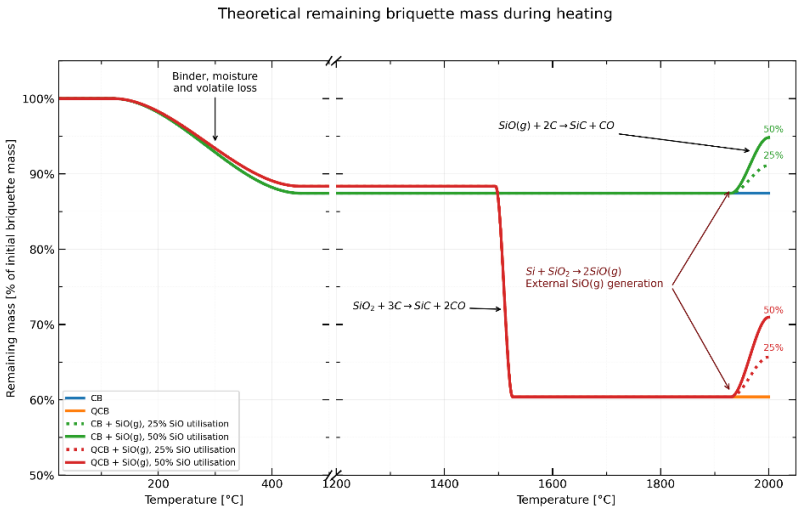

Figure 2: Theoretical remaining briquette mass as a function of temperature for CB and QCB briquettes, with and without exposure to externally generated SiO(g). For the SiO-exposed compositions, theoretical curves assuming 25% and 50% utilisation of the externally generated SiO(g) for SiC formation are shown. The three main stages represent moisture and volatile loss, carbothermal reduction of quartz, and additional SiC formation from externally supplied SiO(g).

3.2 Reaction Sequence from the Long Duration Experiments

Three main reaction stages were identified from the combined off-gas, TGA, and mass-change measurements, and are illustrated in the qualitative CO off-gas profile from a long-duration heating experiment (1400–2000°C) shown in *Figure 3*. The CO measurements are interpreted qualitatively, and the evolution of the CO signal relative to the temperature is used to identify the different reaction stages: (1) binder decomposition and devolatilisation below approximately 900°C, (2) internal carbothermal reduction of quartz between approximately 1400°C and 1700°C, and (3) interaction with externally supplied SiO(g) above approximately 1800°C in the SiO-exposure experiments.

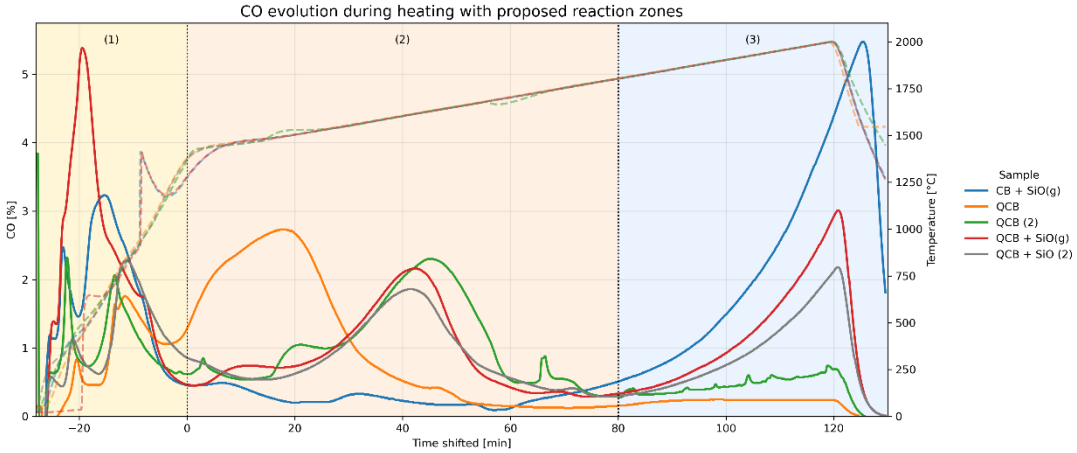

Figure 3: CO off-gas evolution during the long-duration heating experiments, showing the three proposed reaction stages: (1) binder decomposition, (2) carbothermal reduction and SiC formation, and (3) interaction with externally supplied SiO(g). Dashed lines represent the furnace temperature profiles.

3.3 Low-temperature Mass Loss and Binder Decomposition

TGA showed a distinct mass-loss event centred near 300°C for both CB and QCB briquettes, in good agreement with the decomposition range of 280–360°C reported for corn starch (Piglłowska et al., 2020). Total low-temperature mass loss was 13.2 wt.% for CB and 13.1 wt.% for QCB, consistent with the estimates presented in *Section 3.1*. The mass curves stabilised at a clear plateau before the onset of carbothermal reactions, confirming that binder-related processes were complete before the main reduction stage. Net mass losses of CB briquettes after furnace heat treatment were in close agreement with TGA values up to 1900°C (*Table I*), confirming no significant additional reactions in the CB system below this temperature.

Table I: Mass loss of CB briquettes after heat treatment at different temperatures, compared with the TGA baseline. The mass loss remains relatively stable between 1400 and 1900°C.

Condition	Mass loss [wt.%]	Difference from TGA [wt.%]
TGA (CB baseline)	13.2	0.0
CB 1400°C	12.1	−1.1
CB 1700°C	13.3	+0.1
CB 1900°C	13.9	+0.7

3.4 Internal Carbothermal Reduction and SiC Formation

Cross-sectional BSE-SEM images of CB briquettes in the as-prepared state and after heat treatment up to 1900°C are shown in *Figure 4*. The microstructure remained largely unchanged across the investigated temperature range, with no significant phase development or pore formation observed. Note that the dark regions are porosity occurring during sample preparation. This is consistent with the XRD results shown in *Table II*, which confirmed the absence of new silicon-containing phases in the CB briquettes at any temperature. Minor graphitisation of the carbon matrix was observed above 1700°C, but no SiC or other reaction products were detected, confirming that the carbon matrix did not undergo significant chemical reactions in the absence of quartz.

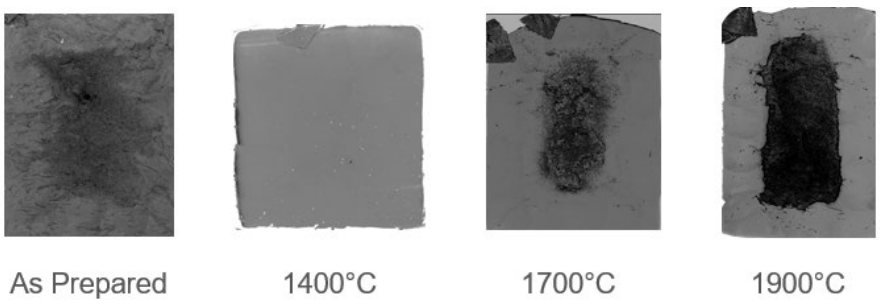

Figure 4: BSE-SEM images of CB briquettes before and after heat treatment, showing limited microstructural change compared with the as-prepared condition. The dark regions correspond to pores, and no significant microstructural changes are observed with increasing temperature

Table II: Phase composition of CB briquettes before and after heat treatment at different temperatures, as determined by XRD. No SiC formation was detected at any temperature.

Temperature [°C]	Phase Composition [wt.%]			
	Amorphous	Graphite 1	Graphite 2	SiC-Cubic
As Prepared	100.00	--	-	-
CB 1400°C	100.00		-	-
CB 1700°C	96.17	1.52	2.31	-
CB 1900°C	97.96	0.07	1.97	-

In contrast, the QCB briquettes underwent significant microstructural changes during heat treatment, as shown in *Figure 5*. At 1400°C, quartz particles are still clearly visible as bright regions distributed throughout the carbon matrix. At 1700°C, these regions have largely disappeared and been replaced by pores and SiC-containing phases. The segmented BSE images illustrate this progression quantitatively, showing the increase in pore fraction and SiC-containing regions with increasing temperature.

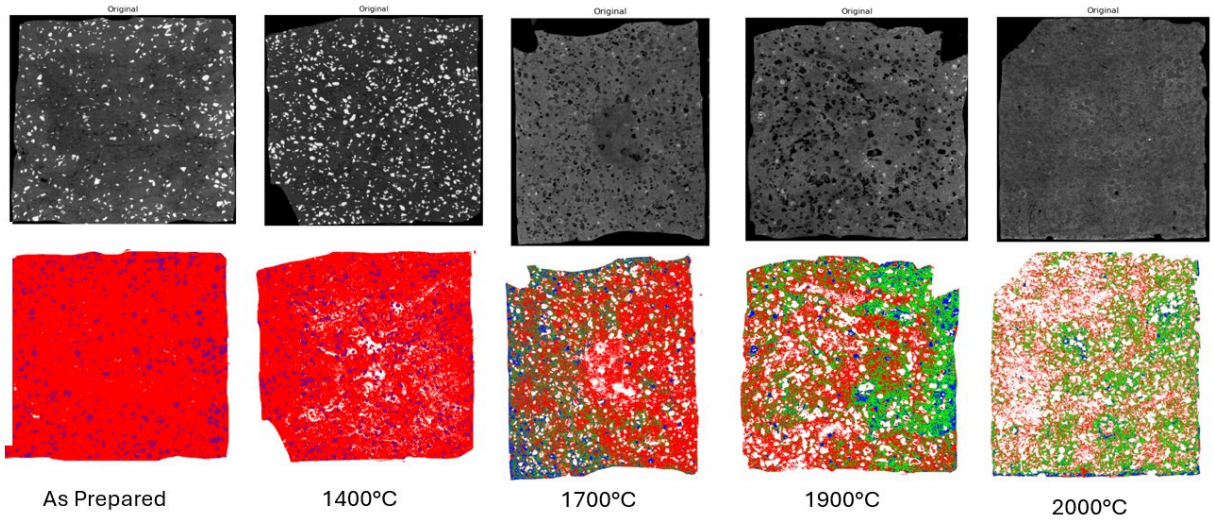

Figure 5: BSE-SEM images and corresponding segmented images from image analysis of QCB briquettes in the as-prepared condition and after heat treatment at 1400°C, 1700°C, 1900°C, and 2000°C. In the segmented images, red represents the carbon phase, purple represents quartz, green represents a mixed SiC–carbon phase, and blue represents SiC clusters.

The XRD results confirm this phase evolution, as shown in Table III. Quartz and cristobalite were detected after heat treatment at 1400°C, whereas no crystalline silica phases were observed at 1700°C and above. The total SiC content at 1700°C reached approximately 22 wt.%, in good agreement with the theoretical value of approximately 20 wt.% expected from complete conversion of the quartz fraction according to *Equation 4*, indicating extensive quartz conversion by 1700°C. The consistently high amorphous fraction across all temperatures is expected to be dominated by unreacted carbon, although a contribution from amorphous silica cannot be excluded based on the XRD results.

Table III: Phase composition of QCB briquettes after heat treatment at different temperatures, as determined by XRD. No crystalline quartz or cristobalite was detected at 1700°C and above, with a corresponding increase in SiC content.

Temperature [°C]	Phase Composition [wt.%]				
	Amorphous	Quartz	Cristobalite	SiC-Cubic	SiC-2H
As Prepared	81.67	18.33	-	-	-
QCB 1400°C	77.98	10.44	9.28	2.30	-
QCB 1450°C[1]	79.69	4.22	6.25	9.04	0.80
QCB 1700°C	77.74	-	-	20.87	1.39
QCB 1900°C	78.96	-	-	17.51	3.53
QCB 2000°C	81.15	-	-	17.67	1.18

[1] *Longer holding time (2 h).*

3.5 Reaction with externally generated SiO(g)

The segmented BSE-SEM images in *Figure 6* illustrate the difference in microstructural response between CB and QCB briquettes exposed to externally generated SiO(g). In both briquette types, SiC formation is concentrated at the bottom and along the sides of the briquette cross-section, as indicated by the blue regions, consistent with SiO(g) entering the briquette from below and reacting with carbon at the exposed surfaces. Both CB and QCB briquettes reacted with externally supplied SiO(g), although the amount of SiO(g) generated differed between experiments, which should be considered when comparing the extent of SiC formation between the two briquette types.

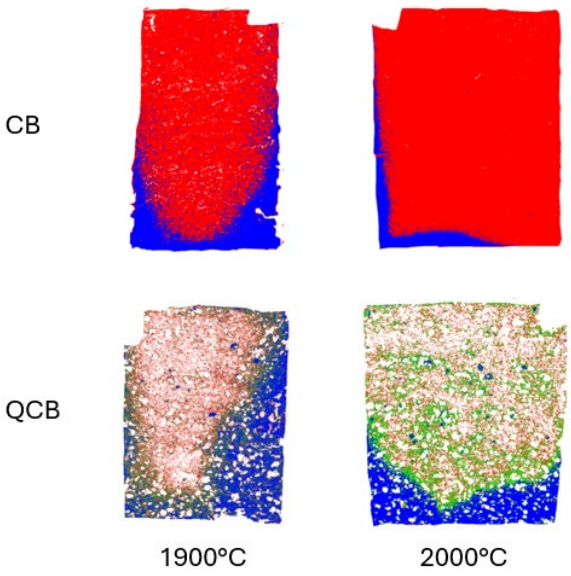

Figure 6: Segmented BSE-SEM images of CB and QCB briquettes after exposure to externally generated SiO(g) at 1900°C and 2000°C. Red represents the carbon phase, green represents a mixed SiC–carbon phase, and blue represents SiC clusters.

The SiO(g) generation and corresponding SiC formation from XRD are summarised in *Table IV*. Exposure to externally generated SiO(g) resulted in additional SiC formation in both briquette types. The additional SiC content (ΔSiC) was calculated relative to the corresponding standard experiments without external SiO(g), and no parallel experiments were conducted, so the values should be interpreted as indicative rather than statistically confirmed. The amount of SiO(g) generated was lower than theoretically expected (Sindland, 2020), suggesting incomplete reaction or SiO losses within the experimental setup.

When normalised to the amount of SiO(g) generated, comparable levels of additional SiC formation were observed for both CB and QCB briquettes, suggesting a comparable ability to react with externally supplied SiO(g). Nevertheless, the QCB briquettes retained a substantial SiO-capture capability despite extensive prior internal reduction, indicating that reactive carbon surfaces remained available for further SiC formation. This is consistent with Li et al. (2018), who reported that good matching between quartz–carbon reactivity and SiO reactivity reduces SiO losses.

Table IV: Estimated SiO(g) generation and corresponding crystalline SiC content in briquettes exposed to external SiO(g). The additional SiC content (ΔSiC) was calculated relative to the corresponding samples treated without external SiO(g).

Condition	SiO generated [g]	SiO generated [%]	SiC without SiO [wt.%]	SiC with SiO [wt%]	ΔSiC [wt.%]
CB 1900°C + SiO(g)	4.05	20.25	0.00	4.39	4.39
CB 2000°C + SiO(g)	3.56	17.8	0.00	8.55	8.55
QCB 1900°C + SiO(g)	5.72	28.6	21.04	29.59	8.55
QCB 2000°C + SiO(g)	5.62	28.1	18.85	28.91	10.06

3.6 Comparison of measured and theoretical mass loss

The measured mass changes are compared with the theoretical mass balance in Figure 7. For both CB and QCB briquettes without external SiO(g), the measured values are in good agreement with the theoretical predictions, indicating that the low-temperature mass loss and carbothermal reduction account for most of the observed weight changes. For the experiments with external SiO(g), the measured mass changes were consistently smaller than the theoretical predictions. Since the theoretical curves assume complete utilisation of the estimated SiO(g) generated, the discrepancy indicates that only a fraction of the generated SiO(g) reacted with the briquettes. This is consistent with transport limitations, incomplete gas–solid contact, and the non-uniform distribution of SiO(g) within the experimental setup, as discussed in *Section 3.5*.

Although the total SiC content was higher in the QCB briquettes than in the CB briquettes, this was primarily a consequence of the internal carbothermal reduction that had already occurred prior to SiO(g) exposure. When normalised to the amount of SiO(g) generated, comparable levels of additional SiC formation were observed for both briquette types, suggesting a similar ability to react with externally supplied SiO(g). Nevertheless, the QCB briquettes retained a substantial SiO-capture capability despite extensive prior internal reduction, indicating that reactive carbon surfaces remained available for further SiC formation.

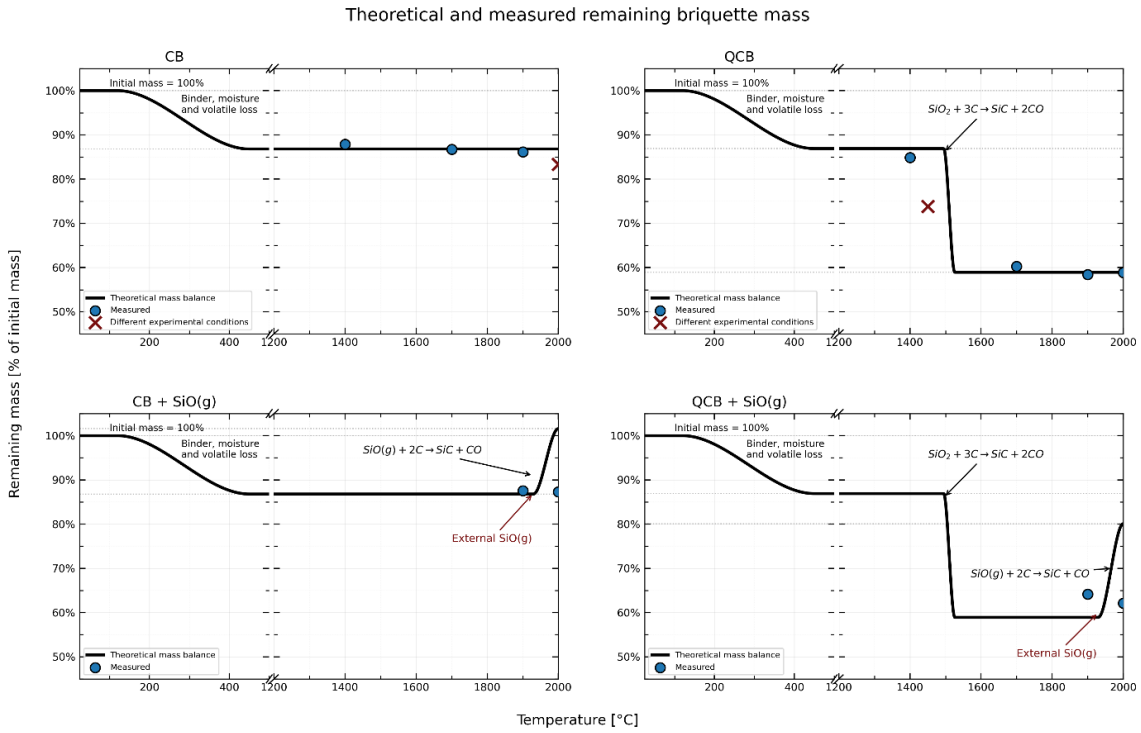

Figure 7: Theoretical and measured remaining briquette mass as a function of temperature for CB and QCB briquettes, with and without exposure to externally generated SiO(g). The theoretical curves assume complete low-temperature volatile loss, full carbothermal reduction of quartz, and complete utilisation of the estimated SiO(g) generated. Measured values are shown as individual data points.

3.7 Future work

The present work investigated a wide range of temperatures and reaction conditions relevant to silicon production. Future studies should focus on obtaining a more detailed understanding of the high-temperature behaviour of these briquettes. During sample handling, the QCB briquettes appeared to exhibit a higher mechanical strength than the CB briquettes once substantial SiC formation had occurred. Although this observation was not quantified, it represents an interesting topic for future investigation through dedicated mechanical strength measurements. Further studies should also investigate whether the increased porosity generated during internal carbothermal reduction contributes to the substantial SiO(g) capture observed in the QCB briquettes by increasing the available reactive surface area.

4. CONCLUSIONS

The high-temperature behaviour of QCB and reference CB briquettes was investigated at temperatures between 1400°C and 2000°C, with and without exposure to externally generated SiO(g). Both briquette types showed an initial mass loss of approximately 13 wt.% below approximately 900°C, attributed to corn starch decomposition, devolatilisation of residual volatile matter, and moisture removal, which were complete before the onset of carbothermal reduction.

The QCB briquettes underwent extensive phase development between 1400°C and 1700°C. SiC formation started at 1400°C, below the thermodynamic equilibrium onset of approximately 1500–1520°C. All crystalline silica phases were consumed by 1700°C, and the total SiC content reached approximately 22 wt.%, in good agreement with the theoretical value of 20 wt.% for complete quartz conversion.

Exposure to externally generated SiO(g) resulted in additional SiC formation concentrated at the bottom and sides of both briquette types, consistent with SiO(g) entering from below. A portion of the generated SiO(g) reacted with both CB and QCB briquettes. Although the QCB briquettes exhibited a greater increase in total SiC content, comparable levels of additional SiC formation were observed for both briquette types when normalised to the amount of SiO(g) generated. The substantial SiO-capture capability observed for the QCB briquettes may be related to the increased porosity developed during internal carbon–quartz reactions at elevated temperatures, which could provide a larger reactive surface area for subsequent reactions with SiO(g).

5. ACKNOWLEDGEMENTS

This work was carried out as part of the QUEEN (Quartz Enrichment Enabling Near-Zero Silicon) project, funded by the European Union's Horizon Europe research and innovation programme.

6. REFERENCES

Haugedal, H. 2025. *The Effects of Biocarbon on Permeability and Wind-Sieving of Charge for Silicon Production*. MSc thesis. Trondheim: NTNU.

Kyaw, T.T. and Tangstad, M. 2024. Use of Agglomerates in Silicon Production. *SSRN Electronic Journal*. doi:10.2139/ssrn.4945352.

Li, F. 2017. *SiC Production Using SiO_2 and C Agglomerates.* PhD thesis. Trondheim: NTNU.

Li, F., Tangstad, M., and Ringdalen, E. 2018. Carbothermal Reduction of Quartz and Carbon Pellets at Elevated Temperatures. *Metallurgical and Materials Transactions B*, 49B, 1078-1088.

Pigłowska, M., et al. 2020. Kinetics and Thermodynamics of Thermal Degradation of Different Starches and Estimation the OH Group and H_2O Content on the Surface by TG/DTG-DTA. *Polymers*, 12(2), 357.

Poch, W. and Dietzel, A. 1962. The Formation of Silicon Carbide from Silicon Dioxide and Carbon. Berichte der Deutschen Keramischen Gesellschaft, 39, 413-426.

Ringdalen, E., Einarsrud, K.E., and Nordhus, A. 2022. Gas Flow and Pressure Drop in Charge Material in Silicon Production. *JOM,* Vol.74, pp.3971-3979.

Schei, A., Tuset, J.K., and Tveit, H. 1998. *Production of High Silicon Alloys*. Trondheim: TAPIR Forlag.

Sindland, C. 2020. *Production Rate of SiO Gas from Industrial Quartz and Silicon*. MSc thesis. Trondheim: NTNU.

Surup, G.R., Trubetskaya, A., and Tangstad, M. 2020. Charcoal as an Alternative Reductant in Ferroalloy Production: A Review. *Processes*, Vol.8, No.11, p.1432.

Wiik, K. 1990. *Kinetics of Reactions Between Silica and Carbon*. Dr.ing. thesis. Trondheim: NTH.

Ingeborg Lillevik Straum

MSc Student, Department of Materials Science and Engineering, NTNU

Ingeborg Lillevik Straum completed her Master's degree in Materials Technology at NTNU in June 2026. Her thesis investigated the high-temperature behaviour of quartz–charcoal briquettes relevant to metallurgical silicon production and was conducted as part of the Horizon Europe QUEEN project. Her research interests include pyrometallurgy, raw material agglomeration, and sustainable production routes for silicon and ferrosilicon.